JCTC Journal of Chemical Theory and Computation

Constant pH Replica Exchange Molecular Dynamics in Biomolecules Using a Discrete Protonation Model

Yilin Meng and Adrian E. Roitberg*

Department of Chemistry and Quantum Theory Project, University of Florida, Gainesville, Florida 32611-8435

Abstract: A constant pH replica exchange molecular dynamics (REMD) method is proposed and implemented to improve coupled protonation and conformational state sampling. By mixing conformational sampling at constant pH (with discrete protonation states) with a temperature ladder, this method avoids conformational trapping. Our method was tested and applied to seven different biological systems. The constant pH REMD not only predicted pK_a correctly for small, model compounds but also converged faster than constant pH molecular dynamics (MD). We further tested our constant pH REMD on a heptapeptide from the ovomucoid third domain (OMTKY3). Although constant pH REMD and MD produced very close pK_a values, the constant pH REMD showed its advantage in the efficiency of conformational and protonation state samplings.

Introduction

Solution pH is a very important thermodynamic variable that affects protein structure, function, and dynamics.[1-3] Many biological phenomena such as protein folding/misfolding,[4-6] substrate docking,[7,8] and enzyme catalysis[9-11] are pH-dependent. Examples include amyloid fibril formation[12] such as misassembly of prion proteins,[13] ATP synthesis,[14] and pH-dependent partial α-helical formation of a 13-residue N-terminal fragment from ribonuclease A.[4,5] This pH-dependence of structure and dynamics comes from changes in the ratio of protonation states for the different residues at different solution pH values.

The pH value at which a particular titratable residue side chain has equal population of protonated and deprotonated states is called the pK_a value of that side chain.[15-18] The pK_a value of a titratable side chain can be highly affected by the environment of that titratable side chain such as protein environment polarity. An ionizable side chain in the interior of a protein can have a different pK_a value from the isolated amino acid in solution.[18] For example, Asp26 of thioredoxin, which lies in a deep pocket of the protein, has a pK_a value of 7.5, while the intrinsic pK_a value of aspartic acid is 4.0.[19] Furthermore, a charged side chain can favor different protonation states in order to stabilize the protein

structure by forming a salt bridge.[20] The conformation and protonation distributions are highly coupled:[21-23] changes in either of them can affect the other one.

Due to the importance of solution pH, Molecular Dynamics (MD) simulations have been used to study its effect on protein structure and dynamics. Other popular theoretical methods developed to calculate (predict) pK_a values include the electrostatic continuum dielectric model and the Poisson−Boltzmann Equation (PBE),[17,24-27] free energy calculation methods,[16,28-30] and empirical methods.[31,32] More details on computer simulation of pK_a prediction and pH dependence of protein structure and dynamics can be found in recent studies.[33-51] The traditional way of studying the effect of pH is setting a constant protonation state before a simulation is carried out. The major problem with this method is that it decouples the correlation between conformation and protonation state, yielding a wrong population of protonation states, especially when the solution pH is close to the pK_a of that titratable site. Furthermore, assigning protonation states before a simulation often involves a guess of protonation state based on our experience.

Constant-pH molecular dynamics (constant-pH MD) methods were developed in order to correlate the protein conformation and protonation state. The purpose of constant-pH MD is to describe protonation equilibrium correctly at a given pH. One category of constant-pH MD methods uses a

* Corresponding author e-mail: roitberg@ufl.edu.

---

continuous protonation parameter. Earlier models include a grand canonical MD algorithm developed by Mertz and Pettitt[52] in 1994 and a method introduced by Baptista et al.[35] in 1997. In the Mertz and Pettitt model, protons are allowed to be exchanged between a titratable side chain and water molecules. Baptista et al. used a potential of mean force to treat protonation and conformation simultaneously. Later, Börjesson and Hünenberger[53,54] developed a continuous protonation variable model in which the protonation fraction is adjusted by weak coupling to a proton bath, using an explicit solvent. More recently, the continuous protonation state model was further developed by the Brooks group.[39–43,55] They called their constant-pH MD algorithm continuous constant-pH molecular dynamics (CPHMD). In the CPHMD method, Lee et al.[55] applied λ-dynamics[56] to the protonation coordinate and used the Generalized Born (GB) implicit solvent model. They chose a λ variable to control the protonation fraction and introduced an artificial potential barrier between protonated and deprotonated states. The potential is a biasing potential to increase the residency time close to protonation/deprotonation states, and it centered at the half-way point of titration ($\lambda = 1/2$). The CPHMD method was then extended by incorporating an improved GB model and replica exchange molecular dynamics (REMD) algorithm for better sampling.[40–43] The applications of CPHMD and replica exchange CPHMD included predicting pK_a values of various proteins,[40] studying proton tautomerism[39] and pH-dependent protein folding and folding intermediates of the villin headpiece domain.[42,43]

In addition to continuous protonation state models, discrete protonation state methods have also been developed to study the pH dependence of protein structure and dynamics.[36,46–49,57–63] The discrete protonation state models utilize a hybrid molecular dynamics and Monte Carlo (hybrid MD/MC) method. Protein conformations are sampled by molecular dynamics, and protonation states are sampled using a Monte Carlo scheme periodically during a MD simulation. A new protonation state is selected after a user-defined number of MD steps, and the free energy difference between the old and the new state is calculated. The Metropolis criterion[64] is used to accept or reject the protonation change. Various solvent models and protonation state energy algorithms were used in discrete protonation state constant pH MD simulations. The Baptista group[36,46–49] used the Poisson–Boltzmann (PB) equation to calculate protonation energies while their MD was done in explicit solvent. Walczak and Antosiewicz[63] also employed the PB equation to determine protonation energy, but they used Langevin dynamics to propagate coordinates between MC steps. Bürgi et al.[57] calculated the transition energy between two protonation states by using thermodynamic integration (TI) method and explicit solvent. More recently, Mongan et al.[62] developed a method combining the GB model[65,66] and the discrete protonation state model. In Mongan's method, the GB model was used in protonation state transition energy as well as solvation free energy calculations. Therefore, solvent models in conformational and protonation state sampling are consistent, and the computational cost is

small. This model was later coupled with accelerated molecular dynamics[67,68] to achieve better conformational sampling.[69] Dlugosz and Antosiewicz also used the discrete protonation state method to study succinic acid[58] and a heptapeptide derived from the ovomucoid third domain (OMTKY3).[60,61] This heptapeptide corresponds to residue 26−32 of OMTKY3 and has the sequence of acetyl−Ser−Asp−Asn−Lys−Thr−Tyr−Gly−methylamine. Nuclear magnetic resonance (NMR) experiments indicated the pK_a of Asp is 3.6, 0.4 pK_a unit lower than the value of blocked Asp dipeptide.[61] In their studies, the conventional molecular dynamics (MD) simulations were carried out to sample peptide conformations. Dlugosz and Antosiewicz sampled protonation states using the PB equation and used analytical continuum electrostatics to treat solvation effects. Their method predicted the pK_a to be 4.24.

Due to the correlation between conformation and protonation sampling, correct sampling of protonation states requires accurate sampling of protein conformations. Hence, generalized ensemble methods[70–73] such as the multicanonical ensemble algorithm,[74,75] simulated tempering,[76] and replica exchange molecular dynamics (REMD)[77] should be used to avoid kinetic trapping which comes from low rates of barrier crossing in constant temperature MD simulations. These methods make the system perform a random walk in temperature or energy space which allows the system under study to easily overcome energy barriers and hence reduces the problem of kinetic trapping. REMD, the MD version of parallel tempering (PT),[78] has the advantage of a-priori known weight factors, such as Boltzmann weights. REMD has been used in many studies of protein structure and dynamics and proven to drastically increase rates of convergence toward a proper equilibrium distribution. Khandogin et al. applied the REMD algorithm to the continuous protonation state constant-pH method and named it REX-CPHMD. They applied REX-CPHMD to pK_a predictions and pH-dependent protein dynamics such as folding and aggregations.[40–43]

In this paper, we present a study of conformation and protonation state sampling using an REMD algorithm on the discrete protonation state model proposed by Mongan et al. We first tested our method on the basis of five dipeptides and a model peptide having the sequence Ala−Asp−Phe−Asp−Ala (ADFDA). The two ends of model peptide ADFDA were not capped, so the two ionizable side chains would have different environments. Then our method was applied to a heptapeptide from OMTKY3, the same heptapeptide that Dlugosz and Antosiewicz studied in their paper.[60,61] Our purpose is to show that the REMD algorithm coupled with a discrete protonation state description can greatly improve pH-dependent protein conformation and protonation state sampling.

Methods

A. Constant-pH MD Algorithm in AMBER. A detailed description of the discrete protonation state model can be found in the paper of Mongan et al.[62] This algorithm employs discrete protonation states, MC sampling of protonation

states, and the use of a GB model in MD and MC. Given a protein with N titratable sites, the discrete protonation state model means protonation states of a protein are described by a vector $\mathbf{n} = (n_1, n_2, ..., n_N)$ where each n_i is some integer representing the protonation state of titratable residue i. In AMBER, five amino acids are designed to be titratable: aspartate, glutamate, histidine, lysine, and tyrosine. For each titratable residue, different protonation states have different partial charges on the side chain. This model also includes syn and anti forms of protons for the aspartate and glutamate side chains as well as the δ and ε proton locations for histidine.

The goal of constant-pH MD is to describe equilibrium between protonated and deprotonated forms correctly at a given pH. In the discrete protonation model, the populations of each form are sampled by the MC method periodically during a MD simulation. At each Monte Carlo step, a titratable site and a new protonation state for that site are chosen randomly, and the transition free energy at this fixed configuration is used to evaluate the MC move.

Considering a titratable site A in a protein environment, its protonated form is protA-H and the deprotonated form is protA$^-$. The equilibrium between the two forms is governed by their free energy difference. This free energy difference is the ensemble average of different configurations. However, the free energy difference cannot be computed by a molecular mechanics (MM) model since the transition between two forms deals with bond breaking/forming and solvation of a proton which involves quantum mechanical effects.

The above problems can be solved by using a reference compound. The reference compound has the same titratable side chain as protA-H but with a known pK_a value ($pK_{a,ref}$). Following Mongan et al.,[62] we assume the transition free energy can be divided into the quantum mechanics (QM) part and the molecular mechanics (MM) part. We further assume that the quantum mechanical energy components are the same between the reference compound and the protA-H. Since the pK_a of the reference compound is known, its transition free energy from the deprotonated form to the protonated form at a given pH is

$$\Delta G_{ref} = k_B T \ln 10 (pH - pK_{a,ref}) \tag{1}$$

So the QM component of the transition free energy can be expressed as

$$\Delta G_{ref,QM} = \Delta G_{ref} - \Delta G_{ref,MM} \tag{2}$$

where $\Delta G_{ref,MM}$ is the molecular mechanics contribution to the free energy of the protonation reaction for that reference compound. In practice, the QM component of the transition free energy also contains errors from MM calculations, so it is actually better called a non-MM component. Since the approximation of the QM component of the transition free energy is

$$\Delta G_{ref,QM} = \Delta G_{protein,QM} \tag{3}$$

then the transition free energy from protA$^-$ to protA-H can be calculated as

$$\Delta G = k_B T \ln 10 (pH - pK_{a,ref}) + \Delta G_{MM} - \Delta G_{ref,MM} \tag{4}$$

where ΔG_{MM} is the molecular mechanics contribution (electrostatic interactions in nature) to the free energy of the protein titratable site. Hence, by using a reference compound, the QM effects are not needed. Effectively, we compute ΔpK_a relative to the reference compound. Computing ΔpK_a can also help canceling some errors introduced by the GB solvation model through the use of $\Delta G_{ref,MM}$. In AMBER, a reference compound is a blocked dipeptide amino acid possessing a titratable side chain (for example, acetyl–Asp–methylamine). Five reference compounds were constructed corresponding to five titratable residues. The values of $\Delta G_{ref,MM}$ for each reference compound are obtained from thermodynamic integration calculations at 300 K and set as internal parameters in AMBER.[62,79] The ΔG_{MM} is calculated by taking the difference between the potential energy with the charges of the current protonation state and the potential energy with the charges of the new protonation state (i.e., ΔG_{MM} is approximately ΔH by averaging over configurations).

The ΔG from eq 4 is used to decide if a MC move in protonation space should be accepted or rejected. If the transition is accepted, MD steps are carried out to sample conformational space in the new protonation state. If the MC attempt is rejected, MD steps are also carried out with no change to the protonation state.

B. Titration Curve and pK_a Prediction Calculation. The titration curve of an ideal titratable site having no interaction with other titratable groups follows the Henderson–Hasselbalch (HH) equation:

$$pK_a = pH - \log\left(\frac{[A^-]}{[HA]}\right) \tag{5}$$

Molecular dynamics runs are assumed to be ergodic; thus the ratio of time that a titratable site spends in protonated and deprotonated states can be used as concentrations. The analytical form of the titration curve can be obtained by exponentiating both sides of the HH equation. A more generalized form of the HH equation which studies an ionizable residue interacting with another one can be written as

$$pK_a = pH - n\log\left(\frac{[A^-]}{[HA]}\right) \tag{6}$$

So the titration curve of an interacting ionizable residue can be expressed as

$$s = \frac{1}{1 + 10^{n(pK_a - pH)}} \tag{7}$$

where s is the fraction of deprotonation and n is the Hill coefficient. A Hill plot, which can be obtained by plotting $\log([A^-]/[HA])$ as a function of pH, is used to study titration behavior. The HH equation (including its generalized form) will be represented as a straight line in a Hill plot. The x intercept is the pK_a value, and the slope is the Hill coefficient which reflects interactions between titratable residues.

C. Replica Exchange Molecular Dynamics (REMD). A detailed description of the REMD algorithm can be found in the papers of Sugita and Okamoto.[77] In REMD, N noninteracting copies (replicas) of a system are simulated at

(A)

(B)
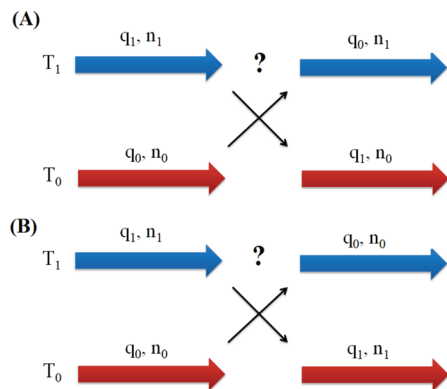
Figure 1. Diagrams displaying exchanging algorithms in constant-pH REMD. (A) Only molecular structures (denoted as *q*) are attempted to exchange. In this case, protonation states are not touched at an exchange attempt. (B) Both molecular structures (denoted as *q*) and protonation states (denoted as *n*) are attempted to exchange at the same time. Metropolis criterion is applied in both algorithms to evaluate transitions.

N different temperatures (one each). Regular molecular dynamics is performed, and periodically an exchange of conformation between two (usually adjacent) temperatures is attempted. Suppose replica *i* at temperature T_n and replica *j* at temperature T_m are attempting to exchange; the following satisfies the detailed balance condition:

$$P_n(i)\, P_m(j)\, w(i \to j) = P_m(i)\, P_n(j)\, w(j \to i) \qquad (8)$$

Here, $w(i{\to}j)$ is the transition probability between two states *i* and *j* and $P_n(i)$ is the population of state *i* at temperature *n* (in REMD assumed Boltzmann weighted). If the Metropolis criterion is applied, the exchange probability is obtained as

$$w(i \to j) = \min\{1, \exp[(\beta_m - \beta_n)(E(q^{[i]}) - E(q^{[j]}))]\} \qquad (9)$$

Here, $q^{[i]}$ is the molecular configuration of state *i*, *E* is the potential energy, and $\beta = 1/k_B T$. If the exchange between two replicas is accepted, the temperatures of the two replicas will be swapped and velocities rescaled to the new temperatures by multiplying all the old velocities by the square root of the new temperature to old temperature ratio:

$$v_{\text{new}} = v_{\text{old}}\sqrt{\frac{T_{\text{new}}}{T_{\text{old}}}} \qquad (10)$$

In the case of constant pH molecular dynamics, the potential energy of the system depends not only on the protein structure but also on the protein protonation state. Likewise, when coupling the REMD algorithm with constant-pH MD, one can either attempt to exchange molecular structures only or swap both structures and protonation states at the same time. For simplicity, let us consider two replicas where replica 0 has temperature T_0, protein structure q_0, and protonation state n_0, while replica 1 has temperature T_1, structure q_1, and protonation state n_1. A diagrammatic description of the two exchange algorithms is shown in Figure 1. The first way of performing an exchange attempt is that replica 0 tries to jump from state (q_0, n_0) to state (q_1, n_0) at temperature T_0 in one Monte Carlo step. Similarly,

replica 1 attempts to transit from state (q_1, n_1) to state (q_0, n_1) at temperature T_1. Protonation states are kept at exchange attempts and only change during dynamics. Therefore, the detailed balance equation now becomes

$$\frac{w(\beta_0 q_0 n_0, \beta_1 q_1 n_1 \to \beta_0 q_1 n_0, \beta_1 q_0 n_1)}{w(\beta_0 q_1 n_0, \beta_1 q_0 n_1 \to \beta_0 q_0 n_0, \beta_1 q_1 n_1)} =$$
$$\frac{\exp(-\beta_0 E(q_0, n_0))\exp(-\beta_1 E(q_1, n_1))}{\exp(-\beta_0 E(q_1, n_0))\exp(-\beta_1 E(q_0, n_1))} \qquad (11)$$

Here, $w(\beta_0 q_0 n_0, \beta_1 q_1 n_1 {\to} \beta_0 q_1 n_0, \beta_1 q_0 n_1)$ is the transition probability of swapping structures. If the Metropolis criterion is used, this exchange probability can be written as

$$w(\beta_0 q_0 n_0, \beta_1 q_1 n_1 \to \beta_0 q_1 n_0, \beta_1 q_0 n_1) = \min\{1, \exp(-\Delta)\} \qquad (12)$$

and

$$\Delta = \beta_0(E(q_0, n_0) - E(q_1, n_0)) - \beta_1(E(q_0, n_1) - E(q_1, n_1)) \qquad (13)$$

where $\beta_0 = 1/k_B T_0$, $\beta_1 = 1/k_B T_1$, and *E* is the potential energy. Here, if the protonation states of two adjacent replicas at an exchange attempt are the same, the exchange probability of our constant pH REMD will be equivalent to the conventional REMD exchange probability. However, if it is not the case, four potential energy terms are needed to calculate exchange probability. Under this circumstance, the constant-pH REMD becomes a REMD algorithm that combines both temperature and Hamiltonian REMD algorithms.

One possible concern of exchanging only structures would be the role of kinetic energy, especially when n_0 and n_1 are different. In the REMD algorithm developed by Sugita and Okamoto, the kinetic energy terms in the Boltzmann factors cancel each other on average through velocity rescaling (eq 10). Only potential energies are required to compute exchange probabilities. There is a problem in canceling kinetic energy terms when the numbers of particles of two systems attempting to exchange are not the same. However, according to the constant-pH MD algorithm proposed by Mongan et al.,[62] a proton does not leave the molecule but becomes a dummy atom when an ionizable side chain is in a deprotonated state. Furthermore, that dummy atom retains its position and velocity, which are controlled by molecular dynamics. Hence, the kinetic energy contributions to the Boltzmann weight will be canceled out during exchange probability calculation, leaving only potential energy useful for the calculation.

The second possibility consists of exchanging protonation states as well as molecular structures at REMD Monte Carlo moves. For instance, replica 0 attempts to move from state (q_0, n_0) to state (q_1, n_1) at temperatures T_0 in one MC move, and replica 1 attempts to jump from state (q_1, n_1) to state (q_0, n_0) at temperature T_1. The detailed balance equation now can be written as

$$\frac{w(\beta_0 q_0 n_0, \beta_1 q_1 n_1 \to \beta_0 q_1 n_1, \beta_1 q_0 n_0)}{w(\beta_0 q_1 n_1, \beta_1 q_0 n_0 \to \beta_0 q_0 n_0, \beta_1 q_1 n_1)} =$$
$$\frac{w(\beta_1 q_1 n_1 \to \beta_1 q_0 n_0)}{w(\beta_1 q_0 n_0 \to \beta_1 q_1 n_1)} \cdot \frac{w(\beta_0 q_0 n_0 \to \beta_0 q_1 n_1)}{w(\beta_0 q_1 n_1 \to \beta_0 q_0 n_0)} \qquad (14)$$

Table 1. The REMD pK_a Predictions of Reference Compounds[a]

pK_a	aspartate	glutamate	histidine	lysine	tyrosine
REMD	3.97 (0.01)	4.41 (0.01)	6.40 (0.03)	10.42 (0.01)	9.61 (0.01)
reference	4.0	4.4	6.5	10.4	9.6

[a] The numbers in parentheses are the standard errors.

This equation states that the exchange probability is the product of MC transition probabilities at temperatures T_0 and T_1. If the protonation states of two adjacent replicas are the same at an exchange attempt, the exchange probability of constant-pH REMD becomes the exchange probability of conventional temperature-based REMD. If n_0 and n_1 are different, then each MC transition is essentially the protonation state change step in constant-pH MD, plus a structural transition. For example, consider the MC transition at temperature T_0

$$w(\beta_0 q_0 n_0 \rightarrow \beta_0 q_1 n_1) = \min\{1, \exp(-\Delta_1)\} \quad (15)$$

where

$$\Delta_1 = \beta_0[E(q_1, n_0) - E(q_0, n_0)] + (\text{pH} - \text{p}K_{a,\text{ref}}) + \beta_0[E_{\text{elec}}(q_1, n_1) - E_{\text{elec}}(q_1, n_0)] - \beta_0 \Delta G_{\text{ref,MM}} \quad (16)$$

The first term in Δ_1 derives from the transition in configuration at fixed protonation state n_0, and the rest corresponds to protonation state change at fixed structure q_1. E_{elec} represents the electrostatic component of potential energy. Similarly, the transition probability of a MC jump at T_1 can be expressed as

$$w(\beta_1 q_1 n_1 \rightarrow \beta_1 q_0 n_0) = \min\{1, \exp(-\Delta_2)\} \quad (17)$$

where

$$\Delta_2 = \beta_1[E(q_0, n_1) - E(q_1, n_1)] - (\text{pH} - \text{p}K_{a,\text{ref}}) - \beta_1[E_{\text{elec}}(q_0, n_1) - E_{\text{elec}}(q_0, n_0)] + \beta_1 \Delta G_{\text{ref,MM}} \quad (18)$$

Therefore, according to eq 14, the exchange probability can be written as

$$w(\beta_0 q_0 n_0, \beta_1 q_1 n_1 \rightarrow \beta_0 q_1 n_1, \beta_1 q_0 n_0) = \min\{1, \exp(-\Delta')\} \quad (19)$$

and

$$\Delta' = \Delta + \beta_0[E_{\text{elec}}(q_1, n_1) - E_{\text{elec}}(q_1, n_0)] - \beta_1[E_{\text{elec}}(q_0, n_1) - E_{\text{elec}}(q_0, n_0)] + (\beta_0 - \beta_1) \cdot \Delta G_{\text{ref,MM}} \quad (20)$$

where Δ is the same quantity as in eq 13.

The exchange probability calculation in the second method of coupling REMD and constant-pH MD utilizes the same number of energy evaluations required by the first method since obtaining electrostatic potential energies does not require extra energy calculations. The advantage of implementing the second exchanging protocol (exchange both structures and protonation states) over the first one (exchange structures only) should not be significant because it is the conformational sampling at higher temperature that greatly improves conformational sampling at lower temperatures. Allowing protonation states to change at exchange attempts does not provide extra gains in conformational sampling since the protonation state space is well sampled during the MD propagation. Therefore, only the first method of performing exchanges was implemented.

D. Simulation Details. For our study, constant pH REMD simulations were carried out first on five reference compounds: blocked aspartate, glutamate, histidine, lysine, and tyrosine, to test our method and implementation. The experimental pK_a values of those reference compounds are known[80] and listed in Table 1. We later performed constant pH REMD simulations on a model peptide ADFDA (Ala−Asp−Phe−Asp−Ala, unblocked termini) and a heptapeptide derived from OMTKY3 (residues 26 to 32 with blocked termini). Four replicas were used in the reference compounds and ADFDA REMD simulations. The temperatures were 240, 300, 370, and 460 K for all six molecules. The pH range for the study of acidic side chains was sampled from 2.5 to 6, and the pH range of histidine is from 5.5 to 8. The basic side chains were titrated from pH 9 to 12. An interval of 0.5 was chosen for all titrations.

Eight replicas were chosen for the heptapeptide with a temperature range from 250 to 480 K. A total of 10 ns was used for each replica in all REMD simulations, and an exchange was attempted every 2 ps. A MC move to change the protonation state was attempted every 10 fs. A second set of REMD runs was done with the same overall conditions but different initial structures in order to check simulation convergence.

To compare conformational and protonation state sampling, 100 ns of constant pH MD simulations were carried out for the aspartate reference compound and ADFDA, at the same pH values as in the REMD runs. For the heptapeptide, one set of 10 ns constant pH MD simulations was done at each pH value simulated by the REMD method.

Constant pH REMD and MD simulations were done using the AMBER 10 molecular simulation suite.[81] The AMBER ff99SB force field[82] was used in all the simulations. The SHAKE algorithm[83] was used to constrain the bonds connecting hydrogen atoms in all the simulations which allowed use of a 2 fs time step. The OBC generalized Born implicit solvent model[66] was used to model the water environment in all our calculations. The Berendsen thermostat,[84] with a relaxation time of 2 ps, was used to keep the replica temperatures around their target values. The salt concentration (Debye−Huckel based) was set at 0.1 M. The cutoff for nonbonded interaction and the Born radii was 30 Å.

E. Cluster Analysis. Cluster analysis was done using the Moil-View program[85] in order to compare conformational sampling.[86,87] The MD and REMD trajectories (having same number of frames) at 300 K and under the same solvent pH were combined following a procedure introduced in the paper of Okur et al. Then, the combined trajectory was clustered on the basis of peptide backbone atoms' root-mean-square

deviations (RMSDs). The population fraction corresponding to each cluster was obtained for MD and REMD simulation. The correlation coefficient values which represent the correlations between MD and REMD cluster population were calculated at each solution pH value by doing linear regression. A high correlation between MD and REMD cluster populations indicates that the structure ensembles are close to each other. This method provides a direct comparison of global conformational sampling between MD and REMD simulations. The same technique was used when studying the convergence of constant pH REMD and MD trajectories. A cluster cutoff RMSD of 1.5 Å is chosen for both ADFDA and the heptapeptide during our analysis.

F. Local Conformational Sampling and Its Convergence to the Final State. In our study, the local conformational sampling was examined by comparing the probability density of the backbone dihedral angle pair (φ, Ψ). Essentially, we are comparing the Ramachandran plot of a residue. Each (φ, Ψ) probability density was computed by binning φ and Ψ angle pairs $10° \times 10°$. These two-dimensional histograms were normalized into populations, and the contours were plotted. The metric used to evaluate (φ, Ψ) probability density convergence was the root-mean-squared deviation (RMSD) between the cumulative (φ, Ψ) histogram and the one produced by using all configurations. Each cumulative histogram was constructed by using (φ, Ψ) pairs up to the current time and following the same algorithm mentioned earlier in this section.

Results and Discussion

A. Reference Compounds. We first applied our constant pH REMD method to the reference compounds. Table 1 shows the pK_a values predicted by REMD simulations (10 ns for each replica) as well as the reference pK_a values. All our pK_a values were calculated by fitting to the HH equation. Agreement between constant pH REMD predictions and the reference values can be seen.

The pH titration curves of the same reference compounds showed agreement between MD (100 ns) and REMD simulations. Figure 2 demonstrates the REMD and MD titration curves of aspartic acid reference compound as an example.

We further studied the convergence of protonation states sampling. REMD and MD protonation fractions were plotted with respect to MC attempts for the aspartate reference compound at all pH values. Figure 3A demonstrates the protonated fraction versus time at pH 4 as one example. According to Figure 3A, it suggests that, although the final pK_a predictions are the same for REMD and MD simulations, the protonation state sampling during REMD simulations clearly converges faster than that in a MD run.

B. Model Peptide ADFDA. The model peptide ADFDA (as zwitterion) was chosen as a more stringent test of our constant pH REMD method. The charged termini will provide a different electrostatic environment for each titratable Asp residue, and hence a correct constant pH REMD model should reflect this difference between titration curves of the two Asp residues. The Asp2 residue is closer to the NH_3^+, so the deprotonated state is favored, and the pK_a value
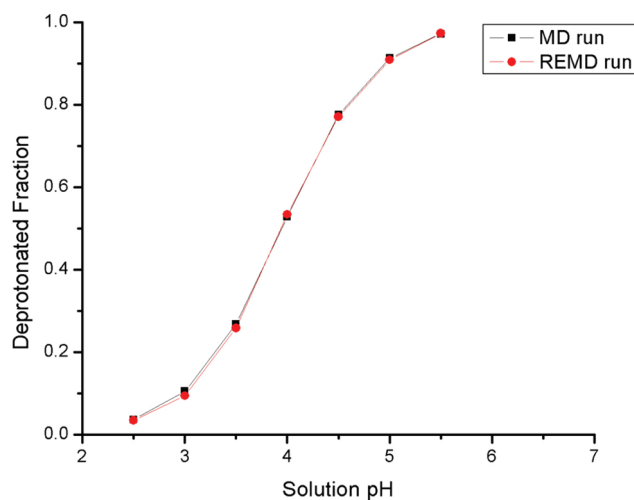

Figure 2. Titration curves of blocked aspartate amino acid from 100 ns MD at 300 K and REMD runs. Agreement can be seen between MD and REMD simulations.
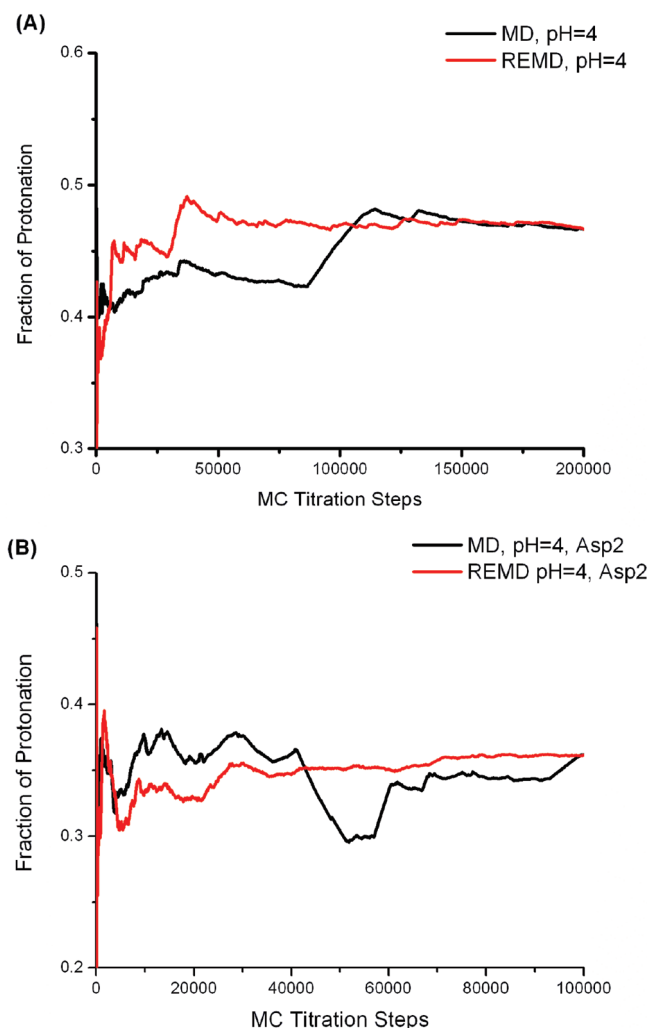
Figure 3. Cumulative average protonation fraction of a titratable residue vs Monte Carlo (MC) steps. (A) Aspartic acid reference compound at pH = 4. (B) Asp2 in model peptide ADFDA at pH = 4.

of Asp2 residue should shift below 4.0 (which is the pK_a of the reference aspartic dipeptide). The Asp4 residue is closer
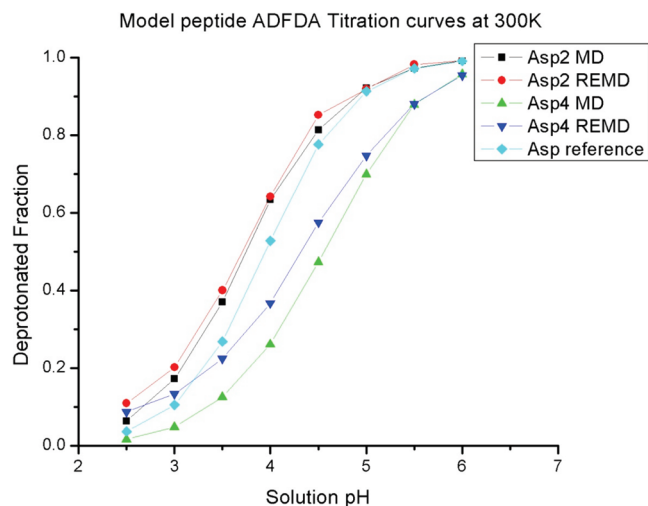
Figure 4. The titration curves of the model peptide ADFDA at 300 K from both MD and REMD simulations. MD simulation time was 100, and 10 ns were chosen for each replica for REMD runs.

Table 2. pK_a Predictions and Hill Coefficients Fitted from the HH Equation

	Asp2		Asp4	
	pK_a	Hill coefficient	pK_a	Hill coefficient
REMD	3.74	0.87	4.38	0.67
MD	3.76	0.89	4.54	0.85

to the COO$^-$ negative charge, and hence the pK_a value should shift above 4.0.

The titration curves of the model peptide ADFDA from REMD simulations are shown in Figure 4. We can clearly see that Asp2 and Asp4 have different titration curves from each other and from the reference compound. The pK_a value and Hill coefficient for each Asp residue were obtained by fitting titration curves to a Hill plot. The results are shown in Table 2. The REMD pK_a predictions reflect the difference between Asp2 and Asp4 due to different peptide electrostatic environments. We also displayed the MD titration curves of Asp2 and Asp4 in Figure 4 and listed the MD pK_a predictions and corresponding Hill coefficients in Table 2. The titration curve of the Asp2 residue only showed a small difference between MD and REMD simulations. But we can see differences in titration behaviors of Asp4 between MD and REMD calculations when the solution pH is below 5. Interestingly, Lee et al. studied blocked Asp−Asp peptide using the CPHMD method,[55] reporting different Hill coefficients for each of the two Asp residues.

Convergence rates of Asp2 titration behavior were compared between REMD and MD calculations due to the fact that Asp2 titration curves are very close. The cumulative protonated fractions versus MC attempts at pH 4 are shown in Figure 3B. Faster convergence in protonation state sampling can be seen for REMD simulation even though both REMD and MD calculations resulted in the same final protonated fraction. Clearly, our constant pH REMD method accelerates the convergence of sampling of protonation states.

In addition to protonation state sampling, we also evaluated the conformational sampling in constant pH MD and REMD
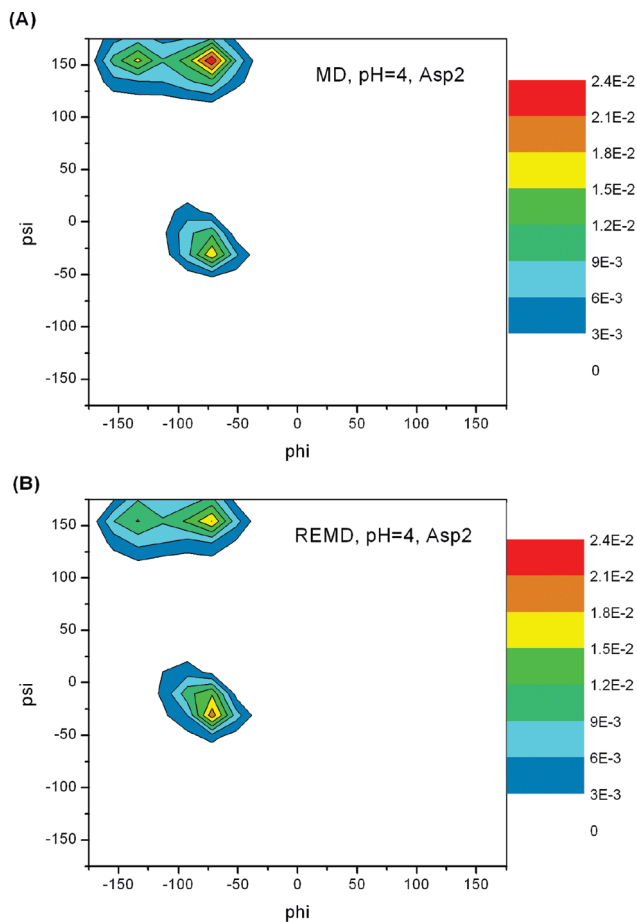
Figure 5. Backbone dihedral angle (φ, Ψ) normalized probability density (Ramachandran plots) for Asp2 at pH 4 in ADFDA. Ramachandran plots at other solution pH values are similar. For Asp2, constant-pH MD and REMD sampled the same local backbone conformational space. Phe3 and Asp4 Ramachandran plots also display the same trend.

Table 3. Correlation Coefficient between MD and REMD Cluster Populations[a]

	pH = 2.5	pH = 3	pH = 3.5	pH = 4
R^2	0.94	0.90	0.79	0.93

	pH = 4.5	pH = 5	pH = 5.5	pH = 6
R^2	0.85	0.98	0.92	0.96

[a] The R^2 values were calculated by linear regression.

simulations. First, distributions of backbone φ and Ψ angle pairs (Ramachandran plots) of residues Asp2, Phe3, and Asp4 in ADFDA at each solution pH were studied. The regions in Ramachandran plots sampled by MD and REMD simulations are the same. Ramachandran plots for residue Asp2 at pH 4 are shown in Figure 5 as an example.

Since the Ramachandran plots only represent local conformational sampling, we also evaluated global conformational sampling by clustering MD and REMD trajectories and comparing the cluster populations. The MD and REMD cluster population R^2 values are listed in Table 3. A plot of cluster populations from MD and REMD trajectories at a solution pH of 4 is shown in Figure 6A as an example. The large R^2 values indicate that the MD and REMD sampled

(A)

(B)
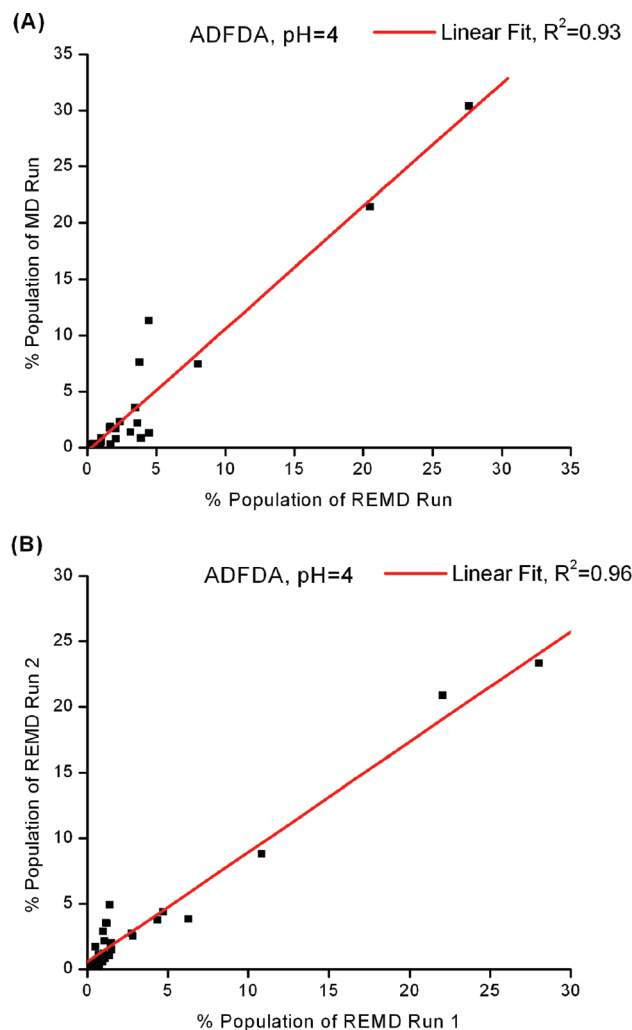
Figure 6. Cluster populations of ADFDA at 300 K. (A) MD vs REMD at pH 4, (B) two REMD runs from different starting structures at pH 4. Large correlation shown in Figure 6B suggests that the REMD runs are converged. Large correlations between two independent REMD runs are also observed at other solution pH values. Correlations between MD and REMD simulations can be found in Table. 3.

the same conformational space and generated the same structure ensemble. The small size of ADFDA and simple structure of each residue make 100 ns long enough for MD to sample the relevant conformations.

We further studied the convergence of REMD simulations by comparing global conformation distribution between two REMD simulations starting from two different structures. Cluster populations of the two REMD simulations at solution pH 4 are displayed in Figure 6B. The R^2 value is 0.959 at pH 4. This large correlation tells us that the two REMD simulations provide the same structure ensemble, and hence the two simulations are converged.

C. Heptapeptide Derived from OMTKY3. We first compared the protonation state sampling between constant pH REMD and MD simulations. Titration curves of Asp3, Lys5, and Tyr7 from two sets of simulations are plotted in Figure 7A and B. For each titratable residue, titration curves generated by constant pH REMD and MD are close to each other. Since the pK_a value of Asp3 in this heptapeptide is

(A)

(B)

(C)
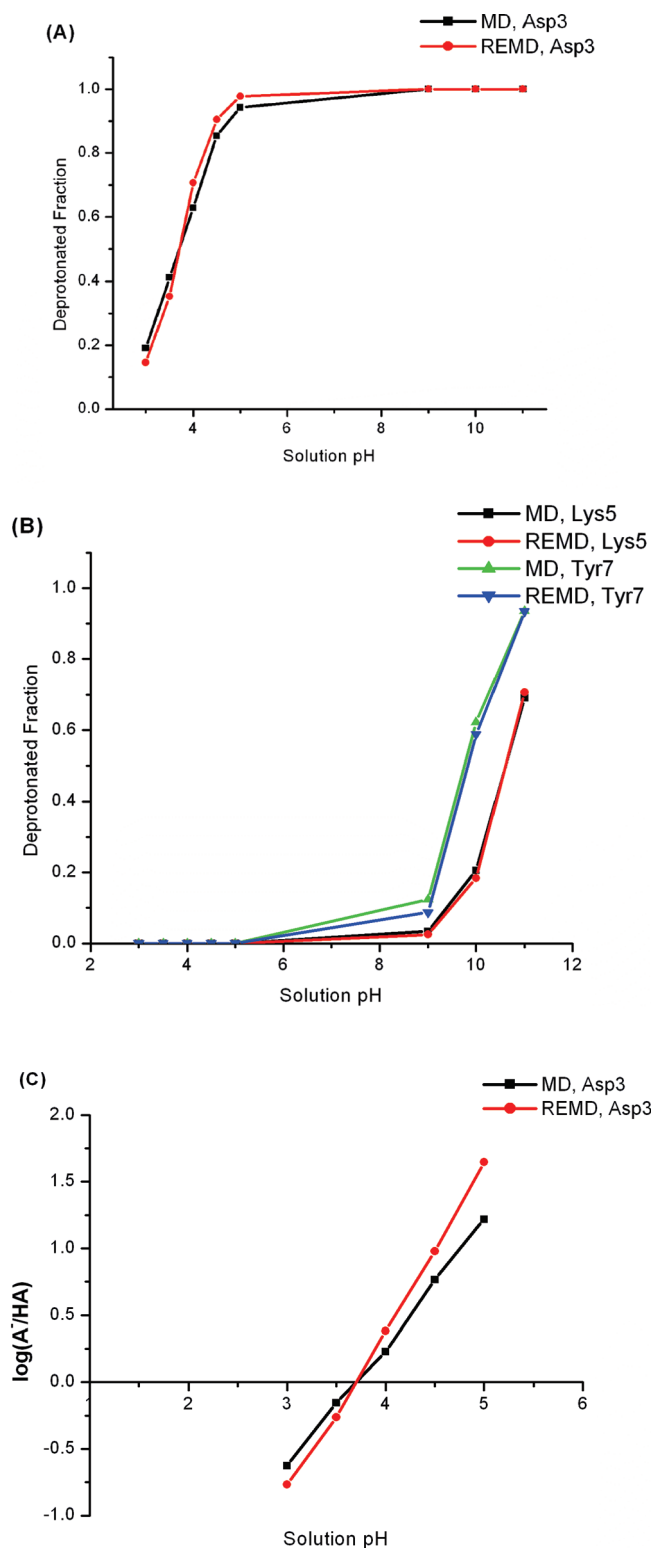
Figure 7. (A and B) Titration curves of Asp3, Lys5, and Tyr7 in the heptapeptide derived from protein OMTKY3. (C) Hill's plots of Asp3. The pK_a values of Asp3 are found through Hill's plots.
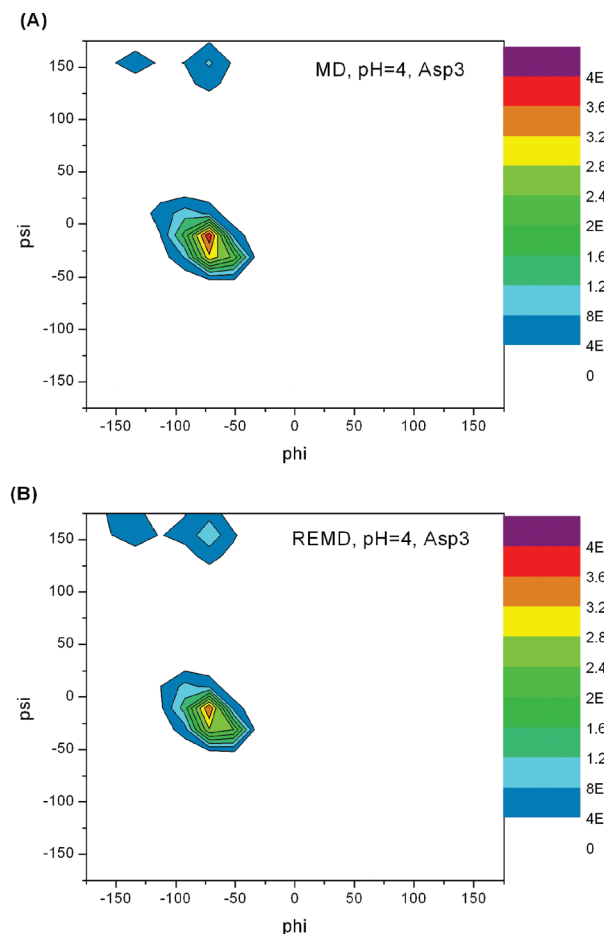
experimentally determined to be 3.6, it will be interesting to evaluate how our predicted values compare to the experimental result. The pK_a values of Asp3 were calculated on the basis of Hill's plots, which are displayed in Figure 7C. The predicted pK_a value is 3.7 for both REMD and MD simulations, and they are in excellent agreement with the

Constant pH Replica Exchange Molecular Dynamics

J. Chem. Theory Comput., Vol. 6, No. 4, 2010 **1409**
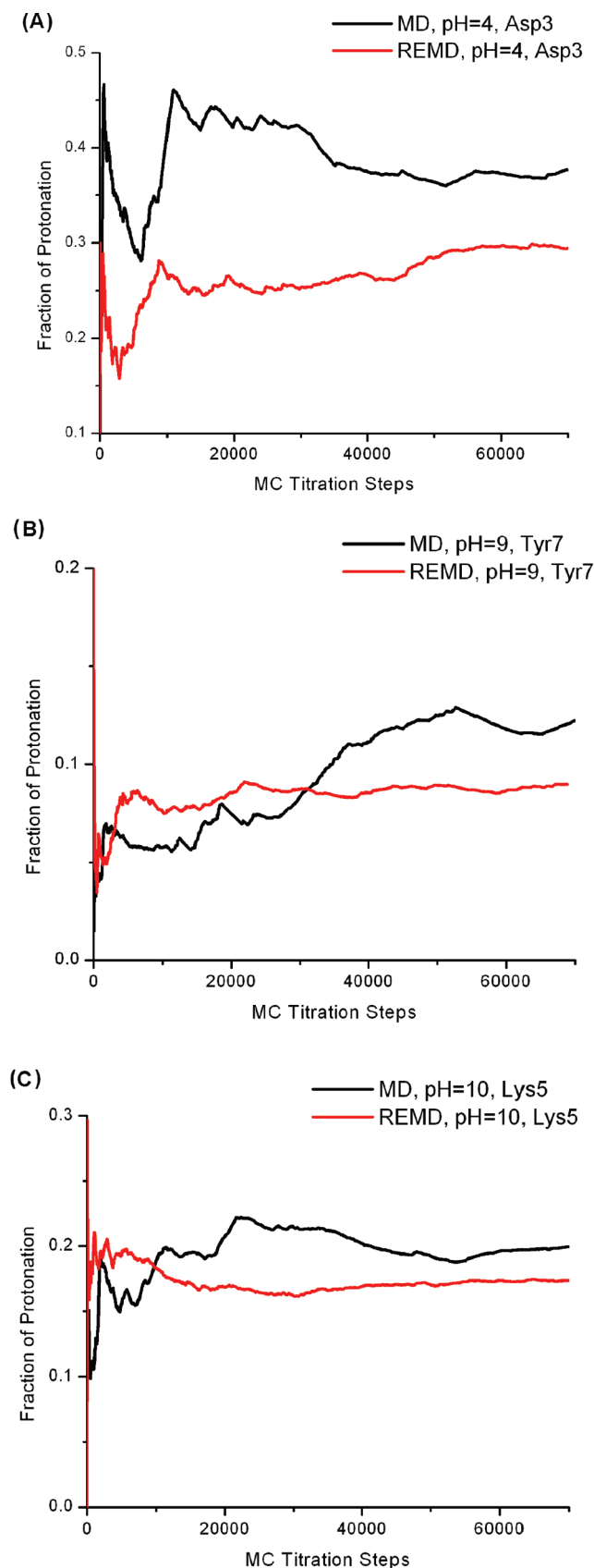
Figure 8. Cumulative average protonation fraction of a titratable residue vs MC steps.

Figure 9. Dihedral angle (φ, Ψ) probability densities of Asp3 at pH 4. (A) Constant-pH MD results; (B) constant-pH REMD results. All others also show a very similar trend.

obtained. Not surprisingly, the REMD and MD schemes yielded essentially the same predicted pK_a values for Lys5 and Tyr7.

Although the final pK_a predictions are the same for constant pH REMD and MD simulations, constant pH REMD showed a clear advantage in the convergence of protonation state sampling. Again, we chose the cumulative average protonation fraction vs MC steps to reflect protonation state sampling convergence for all three titratable residues. Several representative plots are shown in Figure 8. The trend that constant pH REMD simulations produce faster convergence in protonation fraction is universal. Therefore, it is very clear that constant pH REMD method is better than constant pH MD in protonation state sampling.

Conformational sampling is an important issue in constant pH studies. We first looked at the conformational sampling on peptide backbones. We evaluated backbone conformational sampling through Ramachandran plots. Six residues (from Ser2 to Tyr7) are studied here. Not surprisingly, Ramachandran plots from constant pH REMD and MD simulations are very close, suggesting that the overall local conformational samplings are similar. The Ramachandran plots of Asp3 at pH 4 are shown in Figure 9 as examples. The only exception is Tyr7 in acidic pH values. Tyr7 can visit the left-handed α-helix conformation during constant pH REMD runs but is not able to do that in constant pH

experimental pK_a value. Following the same procedures, our predicted pK_a values of Lys5 (10.6 for both REMD and MD) and Tyr7 (9.9 and 9.8 for REMD and MD respectively) were
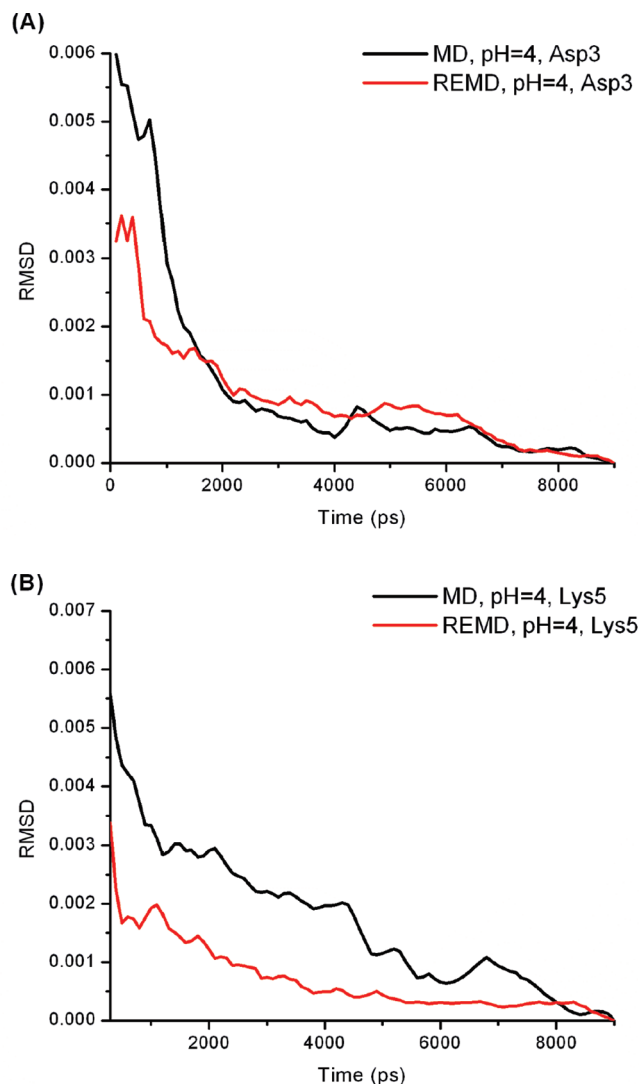
Figure 10. The root-mean-square deviations (RMSDs) between the cumulative (φ, Ψ) probability density up to current time and the (φ, Ψ) probability density produced by the entire simulation. (φ, Ψ) probability density convergence behaviors at other pH values also show that REMD runs converge to final distribution faster.

MD runs. In general, constant pH REMD and MD yielded the same Ramachandran plots for the heptapeptide.

As demonstrated earlier, the overall samplings of (φ, Ψ) distribution by constant pH REMD and MD are similar for Ser2 to Thr6. It is interesting to determine how fast each sampling scheme reaches the final distribution. We studied the evolution of backbone conformational sampling based on cumulative data as we did in the case of protonation state sampling convergence. As described in the Methods subsection F, the RMSD between the (φ, Ψ) probability distribution up to current time versus total simulation time was calculated. The smaller a RMSD is, the closer a probability distribution reaches to the final distribution. Deviations were calculated starting from the second nanosecond with time intervals incremented by 100 ps. The cumulative time-dependence RMSD of Asp3 and Lys5 are also shown in Figure 10 as examples. As seen in the figures, these curves decrease faster in constant pH REMD simulations. Figure 10 suggests that, although the final (φ, Ψ) probability distributions are similar
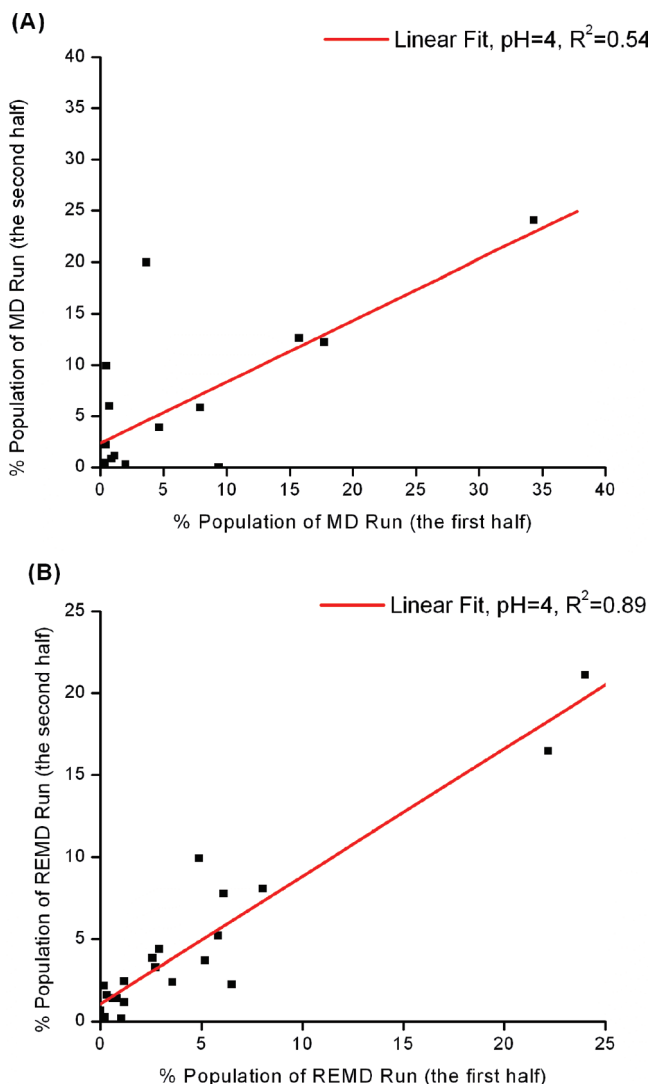
Figure 11. Cluster population at 300 K from constant pH MD and REMD simulations at pH = 4. Cluster analysis is performed using the entire simulation. The populations in each cluster from the first and second halves of the trajectory are compared and plotted. Ideally, a converged trajectory should yield a correlation coefficient to be 1. (A) Constant pH MD. (B) Constant pH REMD. A much higher correlation coefficient can be seen in constant pH REMD simulation, suggesting much better convergence is achieved by the constant pH REMD run.

between constant pH REMD and MD simulations, the constant pH REMD simulation clearly reaches the final state faster.

Cluster analysis was also applied to study the convergence of conformation sampling in the heptapeptide. By comparing cluster populations between the first and second half of one trajectory, one could check the convergence of that simulation. The two halves of a structural ensemble should yield the same populations in each cluster if convergence is reached. For example, for simulations at pH 4, both constant pH REMD and MD yield about 20 clusters, and the correlations coefficients are calculated through a linear regression. Cluster population plots and correlation coefficients are shown in Figure 11. A much higher correlation coefficient can be seen in constant pH REMD simulation,

suggesting the two halves of the constant pH REMD simulation at pH 4 populate each cluster much more similarly than the corresponding constant pH MD does. Hence, much better convergence is achieved by the constant pH REMD run.

Conclusion

In our work, we have applied the replica exchange molecular dynamics (REMD) algorithm to the discrete protonation state model developed by Mongan et al.[62] in order to study pH-dependent protein structure and dynamics. Seven small peptides were selected to test our constant pH REMD method. Constant pH molecular dynamics (MD) simulations were run on the same peptides for comparison. The constant REMD method results are encouraging. The constant REMD method can predict pK_a values in agreement with literature and experimental results. The constant pH REMD method also displays an advantage in convergence behaviors during protonation states and conformational sampling.

The REMD algorithm has been proven beneficial to study pH-dependent protein structures. Our future work will include studies of pH-dependent protein dynamics and application of this constant pH REMD to large proteins.

References

(1) Matthew, J. B.; Gurd, F. R. N.; Garciamoreno, E. B.; Flanagan, M. A.; March, K. L.; Shire, S. J. *Crc Cr. Rev. Bioch. Mol.* **1985**, *18*, 91–197.

(2) Mongan, J.; Case, D. A. *Curr. Opin. Struct. Biol.* **2005**, *15*, 157–163.

(3) Yang, A. S.; Honig, B. *J. Mol. Biol.* **1993**, *231*, 459–474.

(4) Bierzynski, A.; Kim, P. S.; Baldwin, R. L. *Proc. Natl. Acad. Sci. U. S. A.* **1982**, *79*, 2470–2474.

(5) Shoemaker, K. R.; Kim, P. S.; Brems, D. N.; Marqusee, S.; York, E. J.; Chaiken, I. M.; Stewart, J. M.; Baldwin, R. L. *Proc. Natl. Acad. Sci. U. S. A.* **1985**, *82*, 2349–2353.

(6) Schaefer, M.; Van Vlijmen, H. W. T.; Karplus, M. *Adv. Protein Chem.* **1998**, *51*, 1–57.

(7) Antosiewicz, J.; Briggs, J. M.; McCammon, J. A. *Eur. Biophys. J. Biophy.* **1996**, *24*, 137–141.

(8) Hunenberger, P. H.; Helms, V.; Narayana, N.; Taylor, S. S.; McCammon, J. A. *Biochemistry* **1999**, *38*, 2358–2366.

(9) Demchuk, E.; Genick, U. K.; Woo, T. T.; Getzoff, E. D.; Bashford, D. *Biochemistry* **2000**, *39*, 1100–1113.

(10) Dillet, V.; Dyson, H. J.; Bashford, D. *Biochemistry* **1998**, *37*, 10298–10306.

(11) Harris, T. K.; Turner, G. J. *IUBMB Life* **2002**, *53*, 85–98.

(12) Kelly, J. W. *Curr. Opin. Struct. Biol.* **1996**, *6*, 11–17.

(13) Kelly, J. W. *Structure* **1997**, *5*, 595–600.

(14) Rastogi, V. K.; Girvin, M. E. *Nature* **1999**, *402*, 263–268.

(15) Hill, T. L. *J. Am. Chem. Soc.* **1956**, *78*, 3330–3336.

(16) Simonson, T.; Carlsson, J.; Case, D. A. *J. Am. Chem. Soc.* **2004**, *126*, 4167–4180.

(17) Tanford, C.; Kirkwood, J. G. *J. Am. Chem. Soc.* **1957**, *79*, 5333–5339.

(18) Warshel, A. *Nature* **1987**, *330*, 15–16.

(19) Langsetmo, K.; Fuchs, J. A.; Woodward, C. *Biochemistry* **1991**, *30*, 7603–7609.

(20) Eberini, I.; Baptista, A. M.; Gianazza, E.; Fraternali, F.; Beringhelli, T. *Proteins: Struct., Funct., Bioinf.* **2004**, *54*, 744–758.

(21) Sham, Y. Y.; Muegge, I.; Warshel, A. *Biophys. J.* **1998**, *74*, 1744–1753.

(22) Simonson, T.; Archontis, G.; Karplus, M. *J. Phys. Chem. B* **1999**, *103*, 6142–6156.

(23) Warshel, A.; Aqvist, J. *Annu. Rev. Biophys. Biomol. Struct.* **1991**, *20*, 267–298.

(24) Antosiewicz, J.; Mccammon, J. A.; Gilson, M. K. *J. Mol. Biol.* **1994**, *238*, 415–436.

(25) Antosiewicz, J.; McCammon, J. A.; Gilson, M. K. *Biochemistry* **1996**, *35*, 7819–7833.

(26) Bashford, D.; Karplus, M. *Biochemistry* **1990**, *29*, 10219–10225.

(27) Demchuk, E.; Wade, R. C. *J. Phys. Chem.* **1996**, *100*, 17373–17387.

(28) Kamerlin, S. C. L.; Haranczyk, M.; Warshel, A. *J. Phys. Chem. B* **2009**, *113*, 1253–1272.

(29) Riccardi, D.; Schaefer, P.; Cui, Q. *J. Phys. Chem. B* **2005**, *109*, 17715–17733.

(30) Warshel, A.; Sussman, F.; Hwang, J. K. *J. Mol. Biol.* **1988**, *201*, 139–159.

(31) Bas, D. C.; Rogers, D. M.; Jensen, J. H. *Proteins: Struct., Funct., Bioinf.* **2008**, *73*, 765–783.

(32) Li, H.; Robertson, A. D.; Jensen, J. H. *Proteins: Struct., Funct., Bioinf.* **2005**, *61*, 704–721.

(33) Alexov, E. G.; Gunner, M. R. *Biophys. J.* **1997**, *72*, 2075–2093.

(34) Baptista, A. M. *J. Chem. Phys.* **2002**, *116*, 7766–7768.

(35) Baptista, A. M.; Martel, P. J.; Petersen, S. B. *Proteins* **1997**, *27*, 523–544.

(36) Baptista, A. M.; Teixeira, V. H.; Soares, C. M. *J. Chem. Phys.* **2002**, *117*, 4184–4200.

(37) Georgescu, R. E.; Alexov, E. G.; Gunner, M. R. *Biophys. J.* **2002**, *83*, 1731–1748.

(38) Jensen, J. H.; Li, H.; Robertson, A. D.; Molina, P. A. *J. Phys. Chem. A* **2005**, *109*, 6634–6643.

(39) Khandogin, J.; Brooks, C. L. *Biophys. J.* **2005**, *89*, 141–157.

(40) Khandogin, J.; Brooks, C. L. *Biochemistry* **2006**, *45*, 9363–9373.

(41) Khandogin, J.; Brooks, C. L. *Proc. Natl. Acad. Sci. U. S. A.* **2007**, *104*, 16880–16885.

(42) Khandogin, J.; Chen, J. H.; Brooks, C. L. *Proc. Natl. Acad. Sci. U. S. A.* **2006**, *103*, 18546–18550.

1412 *J. Chem. Theory Comput., Vol. 6, No. 4, 2010*

Meng and Roitberg

(43) Khandogin, J.; Raleigh, D. P.; Brooks, C. L. *J. Am. Chem. Soc.* **2007**, *129*, 3056–3057.

(44) Lee, A. C.; Yu, J. Y.; Crippen, G. M. *J. Chem. Inf. Model.* **2008**, *48*, 2042–2053.

(45) Livesay, D. R.; Jacobs, D. J.; Kanjanapangka, J.; Chea, E.; Cortez, H.; Garcia, J.; Kidd, P.; Marquez, M. P.; Pande, S.; Yang, D. *J. Chem. Theory Comput.* **2006**, *2*, 927–938.

(46) Machuqueiro, M.; Baptista, A. M. *J. Phys. Chem. B* **2006**, *110*, 2927–2933.

(47) Machuqueiro, M.; Baptista, A. M. *Biophys. J.* **2007**, *92*, 1836–1845.

(48) Machuqueiro, M.; Baptista, A. M. *Proteins: Struct., Funct., Bioinf.* **2008**, *72*, 289–298.

(49) Machuqueiro, M.; Baptista, A. M. *J. Am. Chem. Soc.* **2009**, *131*, 12586–12594.

(50) Madura, J. D.; Briggs, J. M.; Wade, R. C.; Davis, M. E.; Luty, B. A.; Ilin, A.; Antosiewicz, J.; Gilson, M. K.; Bagheri, B.; Scott, L. R.; Mccammon, J. A. *Comput. Phys. Commun.* **1995**, *91*, 57–95.

(51) Minikis, R. M.; Kairys, V.; Jensen, J. H. *J. Phys. Chem. A* **2001**, *105*, 3829–3837.

(52) Mertz, J. E.; Pettitt, B. M. *Int. J. Supercomput. Ap.* **1994**, *8*, 47–53.

(53) Borjesson, U.; Hunenberger, P. H. *J. Chem. Phys.* **2001**, *114*, 9706–9719.

(54) Borjesson, U.; Hunenberger, P. H. *J. Phys. Chem. B* **2004**, *108*, 13551–13559.

(55) Lee, M. S.; Salsbury, F. R.; Brooks, C. L. *Proteins: Struct., Funct., Bioinf.* **2004**, *56*, 738–752.

(56) Kong, X. J.; Brooks, C. L. *J. Chem. Phys.* **1996**, *105*, 2414–2423.

(57) Burgi, R.; Kollman, P. A.; van Gunsteren, W. F. *Proteins* **2002**, *47*, 469–480.

(58) Dlugosz, M.; Antosiewicz, J. M. *Chem. Phys.* **2004**, *302*, 161–170.

(59) Dlugosz, M.; Antosiewicz, J. M. *J. Phys. Chem. B* **2005**, *109*, 13777–13784.

(60) Dlugosz, M.; Antosiewicz, J. M. *J. Phys.: Condens. Matter* **2005**, *17*, S1607–S1616.

(61) Dlugosz, M.; Antosiewicz, J. M.; Robertson, A. D. *Phys. Rev. E* **2004**, *69*, 021915.

(62) Mongan, J.; Case, D. A.; McCammon, J. A. *J. Comput. Chem.* **2004**, *25*, 2038–2048.

(63) Walczak, A. M.; Antosiewicz, J. M. *Phys. Rev. E* **2002**, *66*, 051911.

(64) Metropolis, N.; Rosenbluth, A. W.; Rosenbluth, M. N.; Teller, A. H.; Teller, E. *J. Chem. Phys.* **1953**, *21*, 1087–1092.

(65) Bashford, D.; Case, D. A. *Annu. Rev. Phys. Chem.* **2000**, *51*, 129–152.

(66) Onufriev, A.; Bashford, D.; Case, D. A. *J. Phys. Chem. B* **2000**, *104*, 3712–3720.

(67) Hamelberg, D.; Mongan, J.; McCammon, J. A. *J. Chem. Phys.* **2004**, *120*, 11919–11929.

(68) Hamelberg, D.; Mongan, J.; McCammon, J. A. *Protein Sci.* **2004**, *13*, 76–76.

(69) Williams, S. L.; de Oliveira, C. A. F.; McCammon, J. A. *J. Chem. Theory Comput.* **2010**, *6*, 560–568.

(70) Li, H. Z.; Fajer, M.; Yang, W. *J. Chem. Phys.* **2007**, *126*, 024106.

(71) Mitsutake, A.; Sugita, Y.; Okamoto, Y. *Biopolymers* **2001**, *60*, 96–123.

(72) Zheng, L. Q.; Chen, M. G.; Yang, W. *Proc. Natl. Acad. Sci. U. S. A.* **2008**, *105*, 20227–20232.

(73) Zheng, L. Q.; Chen, M. G.; Yang, W. *J. Chem. Phys.* **2009**, *130*, 234105.

(74) Berg, B. A.; Neuhaus, T. *Phys. Lett. B* **1991**, *267*, 249–253.

(75) Berg, B. A.; Neuhaus, T. *Phys. Rev. Lett.* **1992**, *68*, 9–12.

(76) Lyubartsev, A. P.; Martsinovski, A. A.; Shevkunov, S. V.; Vorontsovvelyaminov, P. N. *J. Chem. Phys.* **1992**, *96*, 1776–1783.

(77) Sugita, Y.; Okamoto, Y. *Chem. Phys. Lett.* **1999**, *314*, 141–151.

(78) Hansmann, U. H. E. *Chem. Phys. Lett.* **1997**, *281*, 140–150.

(79) Case, D. A.; Cheatham, T. E.; Darden, T.; Gohlke, H.; Luo, R.; Merz, K. M.; Onufriev, A.; Simmerling, C.; Wang, B.; Woods, R. J. *J. Comput. Chem.* **2005**, *26*, 1668–1688.

(80) Bashford, D.; Case, D. A.; Dalvit, C.; Tennant, L.; Wright, P. E. *Biochemistry* **1993**, *32*, 8045–8056.

(81) Case, D. A.; Darden, T. A.; Cheatham, I.; Simmerling, C. L.; Wang, J.; Duke, R. E.; Luo, R.; Crowley, M.; Walker, R. C.; Zhang, W.; Merz, K. M.; B.Wang; Hayik, S.; Roitberg, A.; Seabra, G.; Kolossváry, I.; Wong, K. F.; Paesani, F.; Vanicek, J.; Wu, X.; Brozell, S. R.; Steinbrecher, T.; Gohlke, H.; Yang, L.; Tan, C.; Mongan, J.; Hornak, V.; Cui, G.; Mathews, D. H.; Seetin, M. G.; Sagui, C.; Babin, V.; Kollman, P. A. *AMBER 10*; University of California: San Francisco, 2008.

(82) Hornak, V.; Abel, R.; Okur, A.; Strockbine, B.; Roitberg, A.; Simmerling, C. *Proteins: Struct., Funct., Bioinf.* **2006**, *65*, 712–725.

(83) Ryckaert, J. P.; Ciccotti, G.; Berendsen, H. J. C. *J. Comput. Phys.* **1977**, *23*, 327–341.

(84) Berendsen, H. J. C.; Postma, J. P. M.; Vangunsteren, W. F.; Dinola, A.; Haak, J. R. *J. Chem. Phys.* **1984**, *81*, 3684–3690.

(85) Elber, R.; Roitberg, A.; Simmerling, C.; Goldstein, R.; Li, H. Y.; Verkhivker, G.; Keasar, C.; Zhang, J.; Ulitsky, A. *Comput. Phys. Commun.* **1995**, *91*, 159–189.

(86) Okur, A.; Roe, D. R.; Cui, G. L.; Hornak, V.; Simmerling, C. *J. Chem. Theory Comput.* **2007**, *3*, 557–568.

(87) Okur, A.; Wickstrom, L.; Layten, M.; Geney, R.; Song, K.; Hornak, V.; Simmerling, C. *J. Chem. Theory Comput.* **2006**, *2*, 420–433.